CRYSTAL GROWTH & DESIGN
2008
VOL. 8, NO. 9
3160–3164

Boron Carbide and Silicon Oxide Hetero-nanonecklaces via Temperature Modulation

Jifa Tian,[†] Xingjun Wang,[†] Lihong Bao,[†] Chao Hui,[†] Fei Liu,[†,‡] Tianzhong Yang,[†] Chengmin Shen,[†] and Hongjun Gao*[,†]

Beijing National Laboratory for Condensed Matter Physics, Institute of Physics, Chinese Academy of Sciences, Beijing 100080, P. R. China, and State Key Laboratory of Optoelectronic Materials and Technologies, School of Physics and Engineering, Sun Yat-sen University, Guangzhou 510275, P. R. China

Received May 8, 2007; Revised Manuscript Received April 23, 2008

ABSTRACT: Boron carbide and silicon oxide (BCSiO) hetero-nanonecklaces have been successfully synthesized via temperature modulation. This kind of nanostructure was formed by coating 100−500 nm silicon oxide nanoballs onto 20−30 nm boron carbide nanowires. Synthetic analysis shows that a two-step model at different temperatures and the poor wettability between boron carbide and silicon oxide play important roles in the growth of hetero-nanonecklaces. Photoluminescence of the synthesized BCSiO hetero-nanonecklaces shows enhanced visible light emissions at 637.6 nm, which is attributed to the small size of the boron carbide nanowires and defects induced by silicon oxide sheaths.

Introduction

One-dimensional (1D) nanostructures have shown great potential as unique building blocks for fabrication of advanced electronic devices, including field-effect transistors (FETs),[1–3] logic circuits,[4] inverters[5] and decoders.[6] Due to the enhanced mobility from the 1D confinement, two classes of materials, carbon nanotubes and semiconductor nanowires,[7,8] have been studied widely for electronic device applications,[9–11] among which modulated carbon nanotubes or semiconductor nanowires (hetero-nanostructures) are of particular interest. In these 1D hetero-nanostructures, the composition and doping are varied on the nanometer scale, which may enable new and unique electron transport properties for integration in novel functional nanosystems. Some work on 1D hetero-nanostructures with modulated compositions and interfaces has been successfully achieved, for example, nanowire heterojunctions, superlattice nanowires, core−sheath coaxial nanowires, and metal−insulator nanocables.[12–18] Despite this progress, very little work has been reported on hetero-nanonecklaces,[19,20] and especially rational control of size, shape, and geometrical arrangement of the hetero-nanostructures still has not been achieved. Here we report the synthesis and photoluminescence of a functional hetero-nanostructure, silicon oxide and semiconductor boron carbide hetero-nanonecklaces.

Boron carbide, which exhibits high strength and Young's modulus, is one of the important lightweight and high-temperature refractory materials with a melting point exceeding 2400 °C.[20–22] Therefore, boron carbide can be applied in wear-resistant ceramics for usage in extreme conditions, for neutron absorbence in the nuclear industry, and for high-temperature thermoelectric energy conversion. One-dimensional nanostructures of B_4C have been synthesized by several routes, including using carbon nanotubes to react with boron oxide vapor,[23–25] the plasma-enhanced chemical vapor deposition method,[26] porous alumina template,[27] and carbon thermal evaporation.[28,29] Silicon oxide, the surface of which is accessible to be modified specifically and which has relatively low melting temperature, is one of the candidates for photoluminescent, biocompatible, and interface insulation materials.[30] Multicomponent nanostructures of boron carbide and silicon oxide would show unique physical and chemical properties and should have great potential as device elements in architectures for functional nanosystems. For example, the tuned photoluminescence emission from the multicomponent structures or metal-oxide−semiconductor (MOS) transistor arrays can be realized by using boron carbide and silicon oxide as semiconductor and oxide units, respectively, through micro- and nanoscale fabrication techniques. So far, no work has been reported on integrating these two functional materials into one kind of nanostructure. In our work, we synthesized boron carbide and silicon oxide (BCSiO) hetero-nanonecklaces by utilizing the poor wettability between these two materials and controlling their nucleation conditions at different temperature regions. The special nanostructure provides periodic semiconductor−oxide units for incorporation of different functionalities into a nanoscale system.

Experimental Section

Fe_3O_4 nanoparticles with diameter 6−8 nm were synthesized by high-temperature solution-phase reaction of iron(III) acetylacetonate with 1,2-dodecandiol in the presence of oleic acid and oleylamine.[31] Boron powder, boron oxide (B_2O_3), carbon black, and silicon powder were the source materials, and they were mixed adequately with a mass ratio of 2:1:1:1. A silicon(111) wafer uniformly covered by 6−8 nm Fe_3O_4 nanoparticles was used as the substrate. The precursors were put into a ceramic boat, and then the substrate was put on the ceramic boat with the (111) surface facing directly toward the precursors. The reaction boat was then placed in the horizontal tube furnace center, and high-purity argon gas was purged at a flow rate of 300 sccm for 0.5 h in advance to remove air. Then the furnace temperature was raised from room temperature to 250 °C at a rate of 17 °C/min and kept for 30 min to get rid of the organic ligand of catalyst and reduce the water remaining in the precursors. After that, the flow rate of carrier gas was changed to 30 sccm, and the temperature was increased to 1100 °C at a rate of 10 °C/min. When the temperature of the furnace center arrived at 1100 °C, it was kept there for 2 h for nanowire growth, and then the furnace was cooled to room temperature naturally. At last, the gray product of BCSiO hetero-nanonecklaces was found on the silicon substrate.

The morphology of the products was obtained on a field-emission-type scanning electron microscope (SEM; XL-SFEG, FEI Corp.). The detailed microstructure of the product was investigated by transmission electron microscopy (TEM), high-resolution transmission electron

* Corresponding author. Phone: (+86) 10-8264-8035. Fax: (+86) 10-62556598. E-mail: hjgao@aphy.iphy.ac.cn.
[†] Chinese Academy of Sciences.
[‡] Sun Yat-sen University.

10.1021/cg0704246 CCC: $40.75
Published on Web 07/23/2008

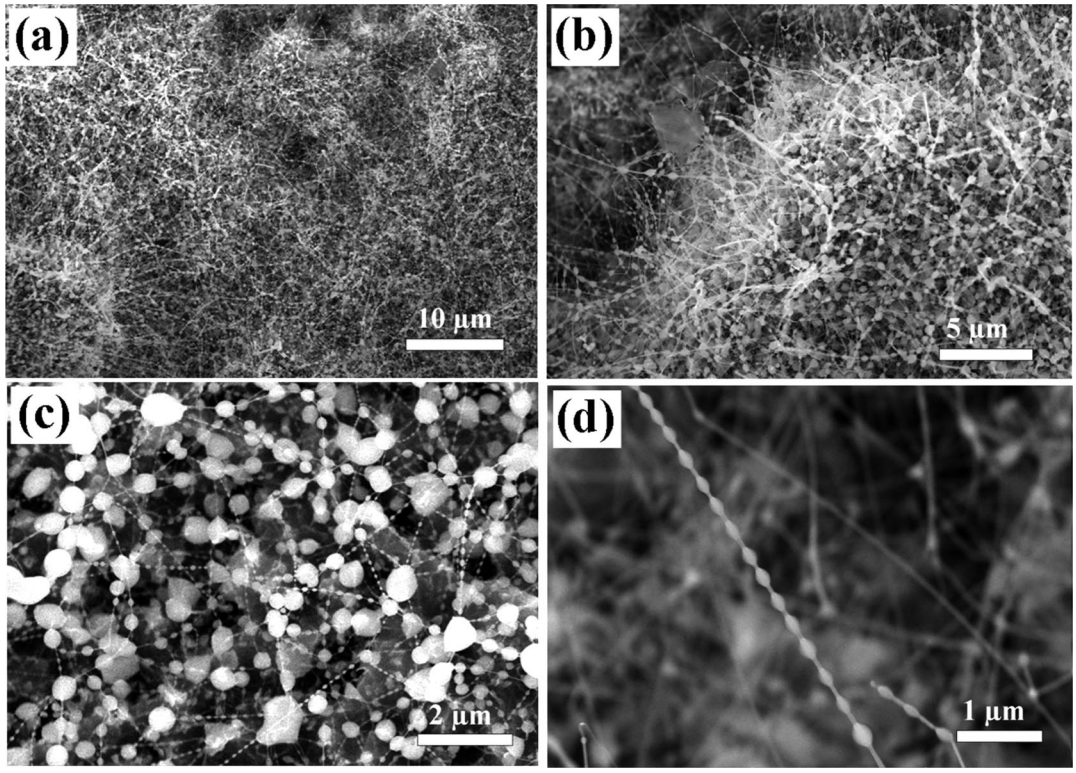

Figure 1. SEM images of boron carbide and silicon oxide hetero-nanonecklaces: (a) low-magnification SEM image of large scale product; (b) local high-magnification SEM image of panel a; (c) SEM image of hetero-nanonecklace network; (d) high-resolution SEM image of single boron carbide and silicon oxide hetero-nanonecklace, showing the silicon oxide nanoballs coated along the boron carbide nanowire at the same distance.

microscopy (HRTEM), and selected area electron diffraction (SAED). Energy-dispersive X-ray spectroscopy (EDS) and electron energy-loss spectroscopy (EELS) were used to identify the chemical compositions of the hetero-nanostructures. Elemental mapping was performed to analyze the elements distribution via a Gatan image filtering (GIF) system attached to the same HRTEM. The photoluminescence measurement was performed on JY-HR800 spectroscopy system.

Results and Discussion

The SEM images of the BCSiO hetero-nanonecklaces are shown in Figure 1. It can be seen that the silicon oxide nanoballs are periodically linked by the boron carbide nanowires. Figure 1a shows the large area assembly of the nanostructure. The higher magnification SEM image (Figure 1b) indicates that the typical structure has a length range from several to several tens of micrometers. Figure 1c reveals that the BCSiO hetero-nanonecklaces with lower density connected by bigger silicon oxide nanoballs have formed a nanonecklace network. These BCSiO nanonecklaces of the network are connected by silicon oxide nanoballs that are three or five times bigger than other nanoballs (Figure 1c). A high-resolution SEM image of a single BCSiO hetero-nanonecklace is shown in Figure 1d. It shows that the BCSiO hetero-nanonecklaces have length of 10 μm. The diameter of the boron carbide nanowires is 20−30 nm, the diameter of the silicon oxide nanoballs is about 100−500 nm, and the nanowires are coated at a distance of 200−300 nm.

TEM images of the BCSiO hetero-nanonecklaces are shown in Figure 2. Two kinds of the structures formed by BCSiO hetero-nanonecklaces can be found in Figure 2a,b. One is the BCSiO hetero-nanonecklace that is composed of a single boron carbide nanowire with several silicon oxide nanoballs (Figure 2a). Another interesting structure shown in Figure 2b is the cross-junctions with two or three hetero-nanonecklaces connected by a bigger silicon oxide nanoball. The inset image in Figure 2a shows the SAED pattern of the boron carbide nanowire, which gives bright sharp diffraction spots and can be indexed to B_4C. The SAED pattern from the silicon oxide nanoballs depicted in the inset of Figure 2b shows a halo-like structure. Figure 2c is the HRTEM image from the nanowire section between two nanoballs. From the corresponding SAED pattern, HRTEM image, and two-dimensional fast Fourier transformation (FFT) of the lattice-resolved image, it is revealed that the central nanowire is rhombohedral B_4C [JCPDF No. 35-0798, space group $R\bar{3}m$ (166), $a = 5.6003$, $c = 12.086$] and its distance of (101) is about 4.499 Å. The HRTEM image from the silicon oxide nanoball is shown in Figure 2d, which cannot give the crystal lattice fringes. Combining the HRTEM images and the corresponding SAED patterns, we conclude that the boron carbide nanowire is single-crystalline and the silicon oxide nanoball is in an amorphous state.

The chemical composition from the different parts of BCSiO hetero-nanonecklace was analyzed by EELS and EDS test (not shown here). Figure 3a shows the typical EELS spectrum of the nanowire section. The characteristic B and C K-edges at 188 and 284 eV are clearly visible. The observed K-edges correspond to sp^2-bonded B and C atoms, with B/C ratio of 4.16, which is consistent with a stoichiometry of B_4C (due to uncertainties in background subtraction and evaluation of pure K-edges, the calculated B/C ratio has an estimated error of 15%). The EELS spectrum from the silicon oxide nanoball only shows Si and O K-edges (Figure 3b). These results confirm that the hetero-nanonecklaces are composed of single-crystalline B_4C nanowires and amorphous SiO_x nanoballs.

To investigate the elemental distribution in BCSiO hetero-nanonecklaces, an energy filter test was carried out. The typical TEM image of BCSiO hetero-nanonecklaces is shown in Figure 4a, where the external surface and interfaces are uniform and

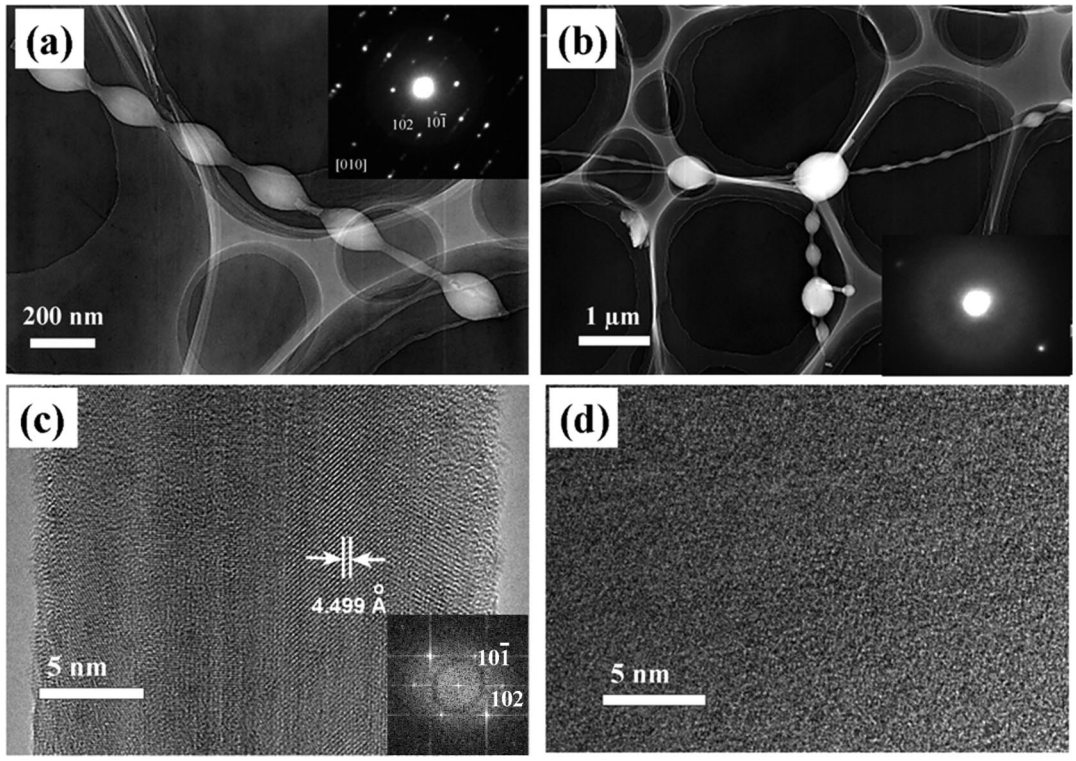

Figure 2. The detailed morphologies and structures of the product: (a) low-resolution TEM image of a single hetero-nanonecklace; the inset is the selected area electron diffraction (SAED) pattern from the central boron carbide nanowire; (b) low-resolution TEM image of a cross-junction of hetero-nanonecklaces; the inset is the selected area electron diffraction from the silicon oxide nanoball; (c) high-resolution TEM image of boron carbide nanowire; (d) high-resolution TEM image of the silicon oxide nanoball.

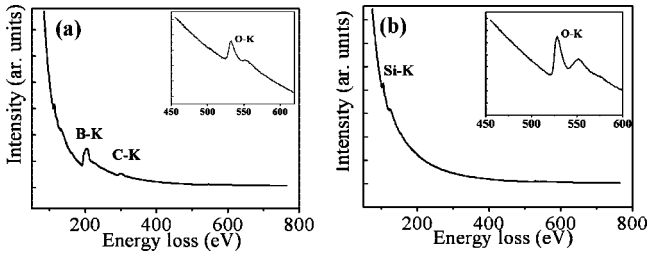

Figure 3. The EELS core electron K-shell spectra from two regions: (a) boron carbide nanowire; (b) silicon oxide nanoball.

clean. Figure 4b is the energy filter mapping image of iron, which shows that there is no iron element in this nanostructure. The energy filter mapping image of boron (Figure 4c) shows that it uniformly located along the longitudinal direction of the BCSiO hetero-nanonecklace. Figure 4d shows a weak profile of the energy filter mapping of carbon located at the same position as boron. Because the concentration of carbon in this hetero-nanostructure is much lower than that of the carbon film of the Cu grid, the mapping profile of carbon is not conclusive. Silicon and oxygen distributed equally in the nanoballs with well-defined compositional profiles from the second nanoball in Figure 4e,f. Notice that silicon only appears on the side surface of the larger nanoball in Figure 4f. This does not mean that silicon is only on the surface, but this is due to the limitation of the EELS mapping (the area of larger nanoball is too thick to get a correct mapping). From Figure 4a, the first nanoball is larger than others, and the signal of silicon was detected only at the position that has the same height of other nanoballs. Actually silicon distributes equally and uniformly in nanoballs. In a word, the hetero-nanojunction is composed of boron carbide nanowires and silicon oxide nanoballs, which is different from the reported hetero-nanostructures.[12–18]

The BCSiO hetero-nanonecklace was obtained by temperature modulation. A two-step growth process at different temperature regions can successfully explain the growth mechanism. In this experiment, the basic reactions employed for the synthesis of hetero-nanonecklaces can be formulated in following equations:

$$B_2O_3(s) \xrightarrow{450\,^\circ C} B_2O_3(l) \quad (1)$$

$$2B_2O_3(l) + 2B \rightarrow 3B_2O_2(l) \quad (2)$$

$$2B_2O_3(l) + 7C \rightarrow B_4C(s) + 6CO(g) \quad (3)$$

$$2B_2O_2(l) + 5C \rightarrow B_4C(s) + 4CO(g) \quad (4)$$

$$CO(g) + B_2O_3(l) + Si \rightarrow B_4C(s) + SiO_2(s) \quad (5)$$

$$(2-x)Si + xSiO_2(s) \xrightarrow{\leq 1000\,^\circ C} 2SiO_x \quad (6)$$

Figure 5 is a schematic illustration of the overall evolution of the growth of boron carbide and silicon oxide hetero-nanonecklaces. The top site of Figure 5 shows the first growth process for synthesis of boron carbide nanowires. This is realized by reactions 1–5 via vapor−liquid−solid (VLS) mechanism.[32] When the temperature of the furnace center is raised to 600−1000 °C, the 6−8 nm Fe_3O_4 nanoparticle catalysts aggregate into 20−40 nm nanoparticles, and adjacent boron carbide vapors are dissolved into these Fe_3O_4 nanoparticles. Once the nearby boron carbide molecules are consumed, the newly coming molecules are adsorbed. Continuous dissolution of boron carbide leads to a supersaturated solution. Boron carbide nanowire growth takes place by precipitation from the

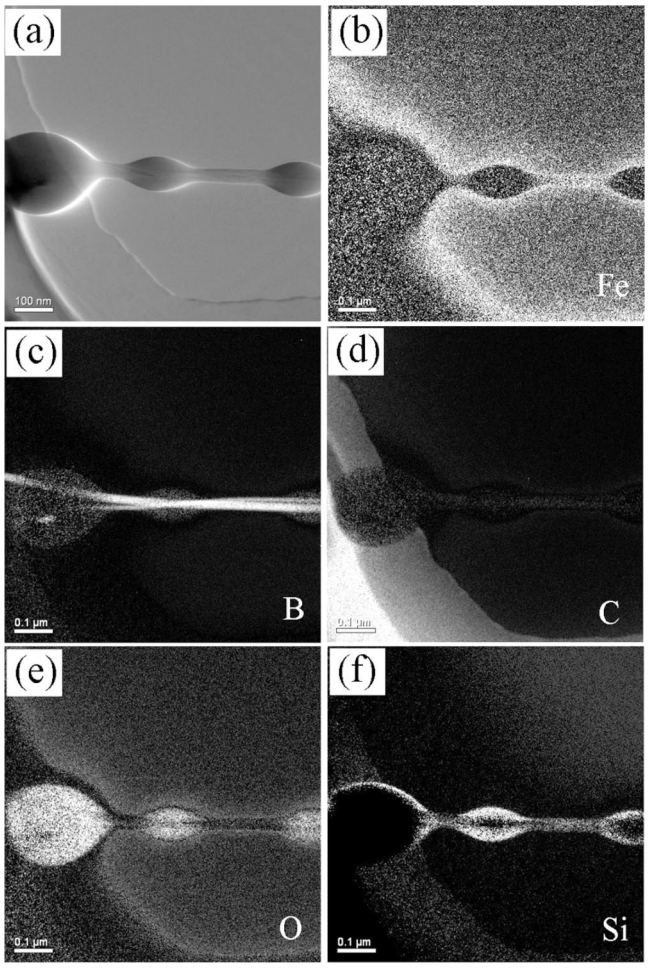

Figure 4. The energy filter mapping results of the boron carbide and silicon oxide hetero-nanonecklace: (a) TEM image of the product; (b) mapping image of iron; (c) mapping image of boron; (d) mapping image of carbon; (e) mapping image of oxygen; (f) mapping image of silicon.

supersaturated liquid of the catalyst center, giving high-density boron carbide nanowires. From the inset SEM and TEM images of the boron carbide nanowires (Figure 5), it can be clearly seen that there is an Fe catalyst cluster at the tip of each nanowire.

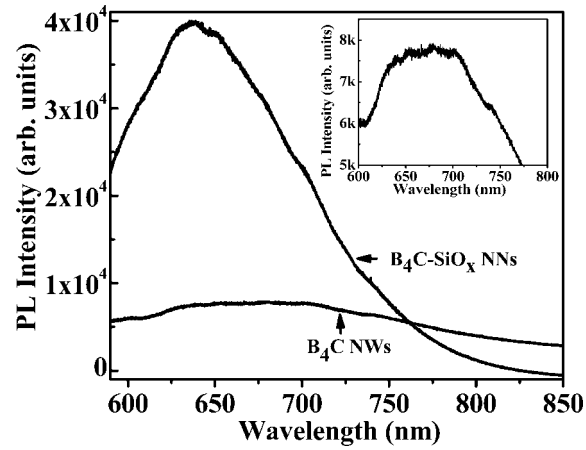

Figure 6. Photoluminescence spectra of boron carbide nanowires and BCSiO hetero-nanonecklace. Inset is the high magnification photoluminescence spectrum of boron carbide nanowires.

The energy filter TEM (EFTEM) analysis of boron carbide nanowire further confirms the VLS growth mechanism (Figure S1, Supporting Information). The coating of silicon oxide nanoballs on the boron carbide nanowires is shown at the bottom site of Figure 5. The formation of SiO_x is dominated by reaction 6. Because the reaction product (SiO_x molecules) is in the vapor state at 1100 °C, after cooling, the saturated vapor pressure of SiO_x molecules decreases and the molecules nucleate at the tip of the boron carbide nanowires. When more and more molecules are adsorbed on this site, some of the liquid silicon oxide flows along the nanowires and covers their surface. But due to the poor wettability between boron carbide and silicon oxide, the silicon oxide shrinks quickly and is separated into several segments, forming silicon oxide nanoballs. At last, the boron carbide and silicon oxide hetero-nanonecklaces were formed.

Figure 6 shows the room temperature photoluminescence (PL) spectra of both BCSiO hetero-nanonecklaces and B_4C nanowires under a 532 nm light excitation source with a power of 3 mW. Notice that the inset is the higher magnification PL spectrum of B_4C nanowires. It indicates that B_4C nanowires show a broad PL emission centered at the wavelength of 660 nm (1.87 eV). The PL emission of bulk boron carbide from the indirect allowed recombination of free excitions[33] is at 1.56 eV (791 nm). It can

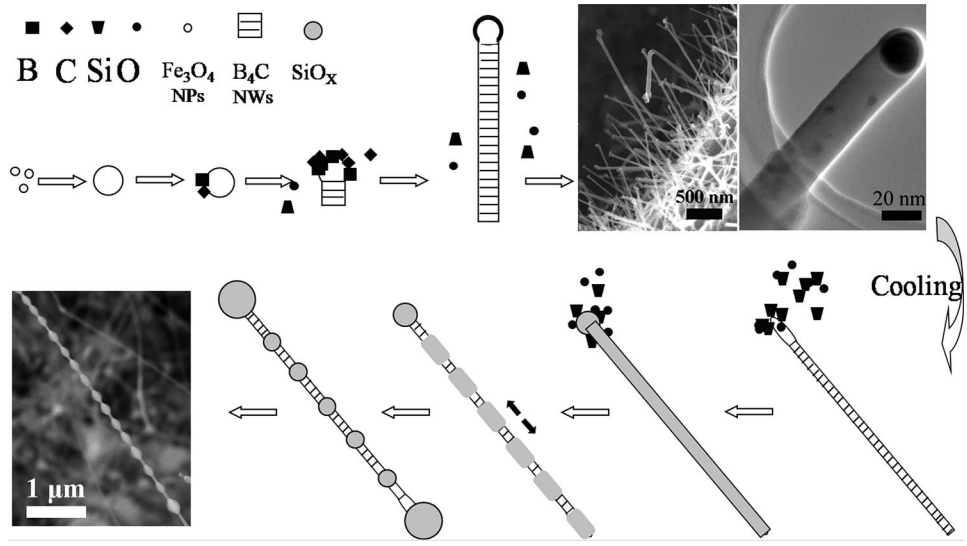

Figure 5. Schematic illustration of the overall evolution of the growth of boron carbide and silicon oxide hetero-nanonecklace.

be speculated that the changes in the electronic structure of semiconductors caused by the quantum size effect lead to blue shift of the PL peak.[34–36] However, for BCSiO hetero-nanonecklaces, a strong visible light emission peak at 637.6 nm was found. The intensity of the emission peak of BCSiO hetero-nanonecklaces was around 5 times stronger than that of boron carbide nanowires. To date, defect state induced emission has been generally accepted to explain the luminescence origin of amorphous silicon oxides. Here, the origin of the PL for BCSiO hetero-nanonecklaces could be due to two possible reasons: the central crystalline boron carbide nanowires with small diameters and the creation of defects in the silicon oxides or the interface boundary.[37–39] In the special hetero-nanonecklaces, the defects of the silicon oxide balls and the oxygen deficiency at the boundary would be increased due to quick formation of the silicon oxide nanoballs and the oxygen-deficiency growth condition. Since these defects are radiative recombination centers, the luminescence intensity is enhanced. The visible emission properties of BCSiO hetero-nanonecklaces are of significant interest for their potential visible emitting device applications.

Conclusions

We reported a two-step route to the synthesis of boron carbide and silicon oxide hetero-nanonecklaces. They are formed by coating 100−500 nm silicon oxide nanoballs onto 20−30 nm boron carbide nanowires. Synthetic analysis shows that temperature modulation and poor wettability between boron carbide and silicon oxide play important roles in the growth of this hetero-nanonecklace. Photoluminescence measurements showed that the BCSiO hetero-nanonecklaces had an intense visible light emission at 637.6 nm. The syntheses will give various 1D composite nanostructures that can be used for both fabrication of advanced nanoelectronic or photonic devices and fundamental understanding of electron transport properties in the structure.

Acknowledgment. This project is supported partially by the National Science Foundation of China (Grant Nos. 90101025 and 60571045) and National "863" (2007AA03Z305) and "973" (2007CB935503) project of China.

Supporting Information Available: The energy filter TEM (EFTEM) analysis of boron carbide nanowires. This material is available free of charge via the Internet at http://pubs.acs.org.

References

(1) Huang, Y.; Duan, X.; Cui, Y.; Lieber, C. M. *Nano Lett.* **2002**, *2*, 101.
(2) Zheng, G.; Lu, W.; Jin, S.; Lieber, C. M. *Adv. Mater.* **2004**, *16*, 1890.
(3) Greytak, A. B.; Lauhon, L. J.; Gudiksen, M. S.; Lieber, C. M. *Appl. Phys. Lett.* **2004**, *84*, 4176.
(4) Huang, Y.; Duan, X.; Cui, Y.; Lauhon, L. J.; Kim, K. H.; Lieber, C. M. *Science* **2001**, *294*, 1313.
(5) Cui, Y.; Lieber, C. M. *Science* **2001**, *291*, 851.
(6) (a) Zhong, Z.; Wang, D.; Cui, Y.; Bockrath, M. W.; Lieber, C. M. *Science* **2003**, *302*, 1377. (b) Yang, C.; Zhong, Z.; Lieber, C. M. *Science* **2005**, *310*, 1304.
(7) Liu, F.; Cao, P. J.; Zhang, H. R.; Tian, J. F.; Xiao, C. W.; Shen, C. M.; Li, J. Q.; Gao, H. J. *Adv. Mater.* **2005**, *17*, 1893.
(8) Wang, X. J.; Tian, J. F.; Yang, T. Z.; Bao, L. H.; Hui, C.; Liu, F.; Shen, C. M.; Gu, C. Z.; Xu, N. S.; Gao, H. J. *Adv. Mater.* **2007**, *19*, 4480.
(9) McEuen, P. L. *Phys. World* **2000**, *13*, 31.
(10) (a) Lieber, C. M. *Sci. Am.* **2001**, (September), 58. (b) Tian, J. F.; Liu, F.; Shen, C. M.; Zhang, H. R.; Yang, T. Z.; Bao, L. H.; Wang, X. J.; Liu, D. T.; Li, H.; Huang, X. J.; Li, J. Q.; Chen, L. Q.; Gao, H. J. *J. Mater. Res.* **2007**, *22*, 1921.
(11) (a) Avouris, Ph. *Acc. Chem. Res.* **2002**, *35*, 1026. (b) Liu, F.; Cao, P. J.; Zhang, H. R.; Shen, C. M.; Wang, Z.; Li, J. Q.; Gao, H. J. *J. Cryst. Growth* **2005**, *274*, 126.
(12) (a) Hu, J. T.; Ouyang, M.; Yang, P. D.; Lieber, C. M. *Nature* **1999**, *399*, 48. (b) Cui, Y.; Lieber, C. M. *Science* **2001**, *291*, 851. (c) Lieber, C. M. *Nano Lett.* **2002**, *2*, 81. (d) Lauhon, L. J.; Gudiksen, M. S.; Wang, D. L.; Lieber, C. M. *Nature* **2002**, *420*, 57.
(13) (a) Wu, Y.; Fan, R.; Yang, P. D. *Nano Lett.* **2002**, *2*, 83. (b) Li, Y.; Ye, C. H.; Fang, X. S.; Yang, L.; Xiao, Y. H.; Zhang, L. D. *Nanotechnology* **2005**, *16*, 501. (c) Wang, X. J.; Tian, J. F.; Bao, L. H.; Hui, C.; Yang, T. Z.; Shen, C. M.; Gao, H. J. *J. Appl. Phys.* **2007**, *102*, 014309.
(14) (a) Bjork, M. T.; Ohlsson, B. J.; Sass, T.; Persson, A. I.; Thelander, C.; Magnusson, K.; Deppert, M. H.; Wallenberg, L.; Samuelson, L. *Nano Lett.* **2002**, *2*, 87. (b) Manna, L.; Scher, E. C.; Li, L. S.; Alivisatos, A. P. *J. Am. Chem. Soc.* **2002**, *124*, 7136.
(15) (a) Hu, J. Q.; Bando, Y.; Liu, Z.; Sekiguchi, T.; Golberg, D.; Zhan, J. *J. Am. Chem. Soc.* **2003**, *125*, 11306. (b) Zhan, J. H.; Bando, Y.; Hu, J. Q.; Liu, Z. W.; Golberg, D. *Angew. Chem., Int. Ed.* **2005**, *44*, 2140.
(16) (a) Ye, C. H.; Zhang, L. D.; Fang, X. S.; Wang, Y.; Yan, P.; Zhao, J. *Adv. Mater.* **2004**, *16*, 1019. (b) Li, Q.; Wang, C. R. *J. Am. Chem. Soc.* **2003**, *125*, 9892.
(17) Wang, X. D.; Song, J. H.; Li, P.; Ryou, J. H.; Dupuis, R. D.; Summers, C. J.; Wang, Z. L. *J. Am. Chem. Soc.* **2005**, *127*, 7920.
(18) (a) Lao, J. Y.; Wen, J. G.; Ren, Z. F. *Nano Lett.* **2002**, *2*, 1287. (b) Bae, S. Y.; Seo, H. W.; Choi, H. C.; Park, J. *J. Phys. Chem. B* **2004**, *108*, 12318.
(19) Ni, H.; Li, X. D. *Appl. Phys. Lett.* **2006**, *89*, 053108.
(20) Inkson, B. J.; Dehm, G.; Peng, Y. *Nanotechnology* **2007**, *18*, 415601.
(21) Wood, C.; Emin, D. *Phys. Rev. B* **1984**, *29*, 4582.
(22) Telle, R. *Structure and Properties of Ceramics, Materials Science and Technology*; VCH: Weinheim, Germany 1994; Vol. 11.
(23) Dai, H.; Wong, E.; Lu, Y.; Fan, S.; Lieber, C. *Nature* **1995**, *375*, 769.
(24) Han, W.; Bando, Y.; Kurashima, K.; Sato, T. *Chem. Phys. Lett.* **1999**, *299*, 368.
(25) Han, W.; Redlich, P.; Ernst, F.; Ruehle, M. *Chem. Mater.* **1999**, *11*, 3620.
(26) Mcllory, D.; Zhang, D.; Cohen, R.; Wharton, J.; Geng, Y.; Norton, M. *J. Mater. Sci. Lett.* **1999**, *18*, 349.
(27) Pender, M.; Sneddon, L. G. *Chem. Mater.* **2000**, *12*, 280.
(28) Carlsson, M.; Carcia-Carcia, F.; Johnson, M. *J. Cryst. Growth* **2002**, *236*, 769.
(29) Ma, R.; Bando, Y. *Chem. Mater.* **2002**, *14*, 4403.
(30) Zhu, Y. Q.; Hu, W. B.; Hsu, W. K.; Terrones, M.; Grobert, N.; Karali, T.; Terrones, H.; Hare, J. P.; Townsend, P. D.; Kroto, H. W.; Walton, D. R. M. *Adv. Mater.* **1999**, *11*, 844.
(31) Yang, T. Z.; Shen, C. M.; Li, Z. A.; Zhang, H. R.; Xiao, C. W.; Chen, S. T.; Xu, Z. C.; Shi, D. X.; Li, J. Q.; Gao, H. J. *J. Phys. Chem. B* **2005**, *109*, 23233.
(32) Wagner, R. S.; Ellis, W. C. *Appl. Phys. Lett.* **1964**, *4*, 89.
(33) Schmechel, R.; Werheit, H.; Kampen, T. U.; Monch, W. *J. Solid State Chem.* **2004**, *177*, 566.
(34) Ekimov, A. I.; Hache, F.; Schanne-Klein, M. C.; Ricald, D.; Flytzanis, C.; Kudryavtsev, I. A.; Yazeva, T. V.; Rodina, A. V.; Efros, Al. L. *J. Opt. Soc. Am. B* **1993**, *10*, 100.
(35) Laheld, V. E. H.; Einevol, G. T. *Phys. Rev. B* **1997**, *55*, 5184.
(36) Nesheva, D.; Raptis, C.; Levi, Z. *Phys. Rev. B* **1998**, *58*, 7913.
(37) Guo, Y. P.; Zheng, J. C.; Wee, A. T. S.; Huan, C. H. A.; Li, K.; Pan, J. S.; Feng, Z. C.; Chua, S. J. *Chem. Phys. Lett.* **2001**, *339*, 319.
(38) Liu, X. M.; Yao, K. F. *Nanotechnology* **2005**, *16*, 2932.
(39) Li, Y.; Ye, C. H.; Fang, X. S.; Yang, L.; Xiao, Y. H.; Zhang, L. D. *Nanotechnology* **2005**, *16*, 501.

CG0704246